

Dalton Transactions

Accepted Manuscript



This is an *Accepted Manuscript*, which has been through the Royal Society of Chemistry peer review process and has been accepted for publication.

Accepted Manuscripts are published online shortly after acceptance, before technical editing, formatting and proof reading. Using this free service, authors can make their results available to the community, in citable form, before we publish the edited article. We will replace this *Accepted Manuscript* with the edited and formatted *Advance Article* as soon as it is available.

You can find more information about *Accepted Manuscripts* in the [Information for Authors](#).

Please note that technical editing may introduce minor changes to the text and/or graphics, which may alter content. The journal's standard [Terms & Conditions](#) and the [Ethical guidelines](#) still apply. In no event shall the Royal Society of Chemistry be held responsible for any errors or omissions in this *Accepted Manuscript* or any consequences arising from the use of any information it contains.

**Core Substituted Naphthalene Diimide – Metallo Bisterpyridine Supramolecular Polymers:
Synthesis, Photophysics and Morphology**

Hamideh Shokouhi Mehr,[‡] Natalie C. Romano,[‡] Rashid Altamimi,[†] Jody M. Modarelli,[§] David
A. Modarelli^{†,*}

A series of metallo Ru(II), Fe(II), Co(II) bisterpyridine polymers were prepared with naphthalene diimide (NDI) groups inserted between two 4'-phenyl-2,2':6',2''-terpyridine (phtpy) groups. Core-substituted NDIs typically have long-lived excited states with relatively high quantum yields, yet the NDI emission in these metallopolymer was completely quenched, most likely because of efficient electron-transfer from the $M(phtpy)_2^{2+}$ groups to the excited NDIs. AFM, TEM and SEM experiments indicate that the regiochemistry of the substitution on the core of the naphthalene diimide, together with coordination of the terpyridine ligand to different metals, strongly influences the morphologies of the resulting metallosupramolecular polymers. The morphologies of spin-coated samples of the *para*-substituted polymers revealed the formation of long, bundled nanorods. Lengths on the order of $\sim 8 \mu\text{m}$ were observed for the bundle of the longest polymers (**5-Ru**) by both AFM and TEM microscopy. The morphologies of the *meta* substituted polymers, on the other hand, exhibited significantly shorter and less well-defined morphologies.

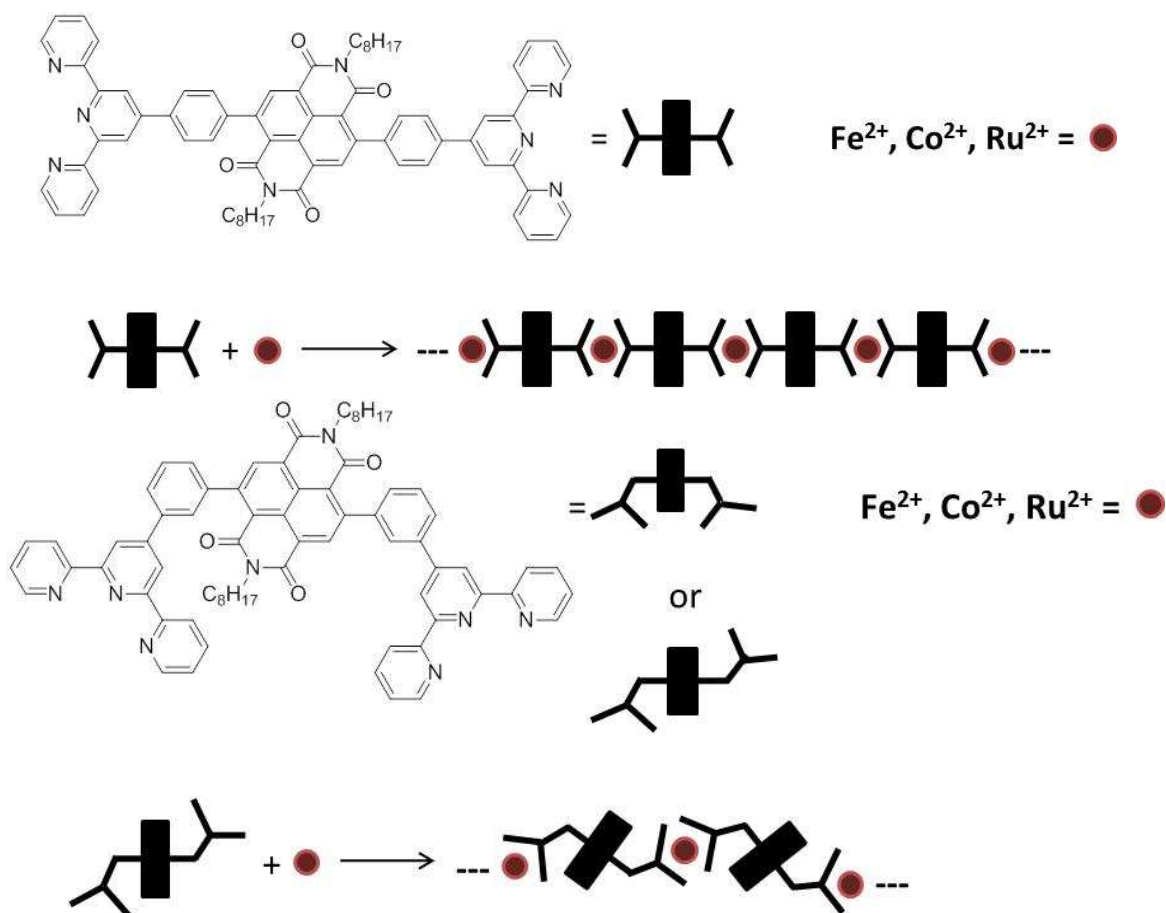
Introduction

Bis(4'-phenyl-2,2':6',2''-terpyridine) (phtpy) based metallosupramolecular polymers^{1,2,3,4,5} have recently attracted great interest^{6,7,8} as a result of their tunable electronic properties that result from changing the metal center, as well as the synthetic advantages that arise from their straightforward preparation. The terpyridine ligand has a high degree of coordination affinity to different transition metal ions that enable the formation of stable metallosupramolecular polymers with well-defined structures and good mechanical and thermal properties.^{3,9} The strong absorption properties of these coordination polymers in the visible region of the absorption spectrum has subsequently led to applications as chemical probes,¹⁰ light emitting devices¹¹ and photosensitizers.¹² Most of these metallosupramolecular polymers have been prepared with simple spacer groups, such as *para*-substituted phenyl and biphenyl groups, between the terpyridine ligands. The incorporation of more complicated spacer groups, such as naphthalene diimides (NDI), can potentially lead to enhanced photophysical and electrochemical properties in the resulting polymers. Core-substituted naphthalene diimides (NDIs) have tunable optical^{13,14} electrochemical,^{15,16} electron transport¹⁷ and anion binding properties.¹⁸ Although the parent unsubstituted NDI does not absorb visible light well, the addition of substituent groups at the core positions shifts the absorption bands markedly to the red.¹³ For example, while NDI has a very weak absorption maximum at 379 nm,^{19,20} the alkoxy core-substituted perylenediimide (PDI) analog displays a significantly red-shifted and more intense absorption band at ~520-540 nm.²¹ The fluorescence properties of NDIs are also markedly changed by core-substitution. While *N,N*-dibutyl-NDI has an emission maximum at 388 nm ($\Phi_{\text{FI}} \sim 0.002$),^{19,22} the core substituted analog has a much more intense red-shifted emission maximum at 567 nm ($\Phi_{\text{FI}} \sim 0.41$).¹³ The incorporation of NDIs into metal terpyridine-based polymers can therefore

potentially add a new dimension to the optical and electrochemical properties of ditopic metallobisterpyridine-based polymers.

A significant amount of work has been performed using the analogous PDI, which has often incorporated into polymers by attachment at either the so-called bay positions or at the imide nitrogens.¹³ However, bay-substituted PDIs must twist out-of-plane in order to avoid steric issues between the PDI ring and the substituent,¹⁵ unlike the planar core-substituted NDI groups, and therefore do not undergo π -stacking as well to form higher order structures. The planar core-substituted NDIs, on the other hand, are highly amenable to the π -stacking interactions that can lead to higher order morphologies.^{23,24,25}

Scheme 1.



In this work, we present the synthesis, characterization, optical properties and self-assembly of metallo ($M = Ru^{2+}$, Fe^{2+} , and Co^{2+}) bisterpyridine polymers with core-substituted naphthalene diimide spacer groups between the terpyridine groups (Scheme 1). We have used transmission electron microscopy (TEM), scanning electron microscope (SEM), and atomic force microscopy (AFM) to determine the morphology of these materials, as well as to measure typical dimensions of the self-assembled structures. The photophysical and electrochemical properties of these polymers have also been investigated by steady state absorption and emission spectroscopies, and cyclic voltammetry (CV).

Experimental

Materials and Methods. Reagents were purchased from TCI-chemical, Sigma-Aldrich, or VWR and were used without further purification. All Suzuki reactions were performed in dry and distilled solvents. NMR spectra (1H , ^{13}C , 2D) were all performed in $CDCl_3$ using either Varian Mercury 300 MHz or 500 MHz spectrometers. Chemical shifts in NMR experiments are reported in parts per million (ppm), while coupling constants (J) are reported in Hertz (Hz). UV-Vis spectra were performed on a Shimadzu Model UV-1601 spectrophotometer with 1.0×10^{-5} M sample concentrations. Emission measurements were carried using an ISA Jobin Yvon SPEX Fluorolog 3-22 fluorometer.

Atomic force microscopy (AFM) was performed using a Veeco Instruments Multimode AFM. Samples for AFM analysis were prepared by rapid spin coating of the polymer on silica surfaces in order to avoid any changes in the polymer lengths or the degree of polymerization upon sample deposition.²⁶ Transmission electron microscopy (TEM) experiments were

performed using a JEOL JSM-1230 microscope at a voltage 120 kV after casting dilute samples in DMF on a 200 mesh carbon-coated Cu grid. Scanning electron microscopy (SEM) measurements were performed using a JEOL JSM-1230 microscope with an accelerating voltage of 0.5-35 kV. Cyclic voltammetry experiments were performed on a Bioanalytical Systems BAS 100B electrochemistry system at 298 K using a gold 0.79 mm² working electrode, a platinum wire auxiliary electrode, and a Ag/Ag⁺ reference electrode. The gold working electrode was rinsed and dried with ethanol and water following polishing with 0.05 μm alumina immediately prior to use. A 0.1 M solution of tetrabutylammonium hexafluorophosphate (TBAPF₆) was used as the supporting electrolyte samples were prepared as 10⁻³ M solutions in dimethylformamide (DMF) as the solvent. All data were collected at a scan rate of 1 V/s. In order to calculate the HOMO and LUMO energy levels of the polymers, the onset potentials of the oxidation and reduction waves were estimated.

2,6-Dibromo-1,4,5,8-naphthalenetetracarboxylic Acid Dianhydride (2). 1,4,5,8-naphthalenetetracarboxylic acid dianhydride **1** (2.0 g, 7.4 mmol) was dissolved in 50 mL oleum (20% SO₃). After stirring for 10 min, a solution of dibromoisocyanuric acid (4.2 g, 14 mmol) and 25 mL oleum (20% SO₃) was added over 4h at room temperature, then the mixture was allowed to stir for 1 h more. The mixture was carefully added to ice to form a light yellow precipitate. The precipitate was filtered and dried under vacuum to a yield yellow solid (3.0 g, 75%), which was used in the next step without further purification.

***N,N'*-Bis(*n*-octyl)-2,6-dibromo-1,4,5,8-naphthalenetetracarboxylic diimide (3).** Dianhydride **2** (2 g, 7.4 mmol) was dissolved in 100 mL of acetic acid and *n*-octylamine (2 ml, 15.4 mmol)

was added to the mixture and heated to 90°C for 4 h. The mixture was cooled to room temperature, poured into ice and then filtered. The resulting light pink solid was chromatographed on silica using CH₂Cl₂/hexane (80:20) to yield **3** as a yellow solid (1.2 g, 60%). ¹H-NMR (400 MHz, CDCl₃): δ 8.77 (s, 2H, Ar-H), 4.19-4.22 (t, 4H, N-CH₂), 1.76 (m, 4H), 1.29-1.53 (m, 20H), 0.87-0.89 (t, 6H), 4.22-4.18 (t, *J* = 7.6 Hz, 4H), 1.79-1.71 (m, 4H), 1.42-1.25 (m, 20H), 0.88-0.86 (t, *J* = 6.4 Hz, 6H).

4'-(4-Boronatophenyl)[2,2':6',2'']terpyridine (4). To a solution of NaOH (3.19 g, 80mmol) in EtOH (120 mL), 4-formylphenylboronic acid (2.0 g, 13.3 mmol) was added and stirred for 1h. 2-Acetylpyridine (3.2 g, 16.6 mmol) was then added to this mixture and stirred overnight, resulting in the formation of a bright yellow precipitate. Aqueous NH₄OH (50-60 mL, 28-30%) was then added and the solution was refluxed for 24 h. Cooling the reaction mixture and washing with CHCl₃ resulted in a white solid (3.7 g, 80%). ¹H NMR (CD₃OD, 300 MHz, ppm): δ 8.68-8.71 (d, 2H, *J* = 4.8 Hz, Py-*H*^{6,6''}), 8.64-8.71 (s, 2H, Py-*H*^{3',5'}), 8.68-8.71 (d, 2H, *J* = 8.1 Hz, Py-*H*^{3,3''}), 7.97-8.03 (dt, 2H, *J* = 8.1, 1.8 Hz, Py-*H*^{4,4''}), 7.71-7.79 (d, *J* = 8.4 Hz, 4H, Ph-*H*), 7.46-7.50 (dd, 2H, *J* = 4.8, 1.8 Hz, Py-*H*^{5,5''}).

2,6-(4'-Diterpyridine)-NDI (5): A solution of diimide **3** (0.2 g, 0.3 mmol) and boronic acid **4** (0.4 g, 0.9 mmol), together with Na₂CO₃ (5 equiv), *tert*-butyl alcohol (7 mL), and PdCl₂(PPh₃)₂ (50 mg) in toluene (25 mL) and water (25 mL) was degassed thrice and purged with N₂ in a Schlenk line and then refluxed for 24 h under nitrogen until the solution turned dark purple color. After cooling to room temperature, the organic layer was extracted with CHCl₃ and dried over MgSO₄. The sample was then concentrated under vacuum and the residue chromatographed on

silica with CH₂Cl₂/hexane (80:20) to form a yellow solid (0.12 g, 40%). ¹H NMR (500 MHz, CDCl₃, ppm): 8.85 (s, 4H, tpy-*H*^{3',5'}), 8.75-8.76 (d, *J* = 2.4 Hz, 4H, tpy-*H*^{6,6''}), 8.68-8.70 (d, *J* = 4.5 Hz, 4H, tpy-*H*^{3,3''}), 8.63 (s, 2H, NDI-H), 8.09-8.11 (d, *J* = 8 Hz, 4H, Ph-*H*), 7.86-7.90 (t, 4H, tpy-*H*^{4,4''}), 7.61-7.62 (d, *J* = Hz, 4H, Ph-*H*), 7.2-7.3 (t, 4H, tpy-*H*^{5,5''}), 4.02-4.05 (t, 4H, N-CH₂), 1.66 (m, 9H), 1.26-1.28 (m, 20H), 0.86 (m, 6H). ¹³C NMR (125 MHz, CDCl₃, ppm): 156.46, 156.00, 150.01, 149.21, 148.72, 142.29, 137.44, 137.11, 136.52, 133.43, 130.65, 128.79, 128.14, 127.70, 127.23, 123.94, 121.59, 119.06, 117.72, 71.82. MALDI-ToF MS (*m/z*): Calcd. for [C₇₂H₆₄N₈O₄]⁺: 1105.33; Found: 1106.3321 [M+H]. UV-Vis in CHCl₃: λ_{max} 380 nm (*ε* = 5 × 10⁵ M⁻¹ cm⁻¹) and λ_{max} 287 nm (*ε* = 1.0 × 10⁵ M⁻¹ cm⁻¹).

4'-(3-Boronatophenyl)[2,2':6',2'']terpyridine (6). To a solution of NaOH (3.19 g, 80 mmol) and EtOH (120 mL), 3-formylphenylboronic acid (2.0 g, 13.3 mmol) was added and stirred for 1 h. 2-Acetylpyridine (3.2 g, 16.6 mmol) was then added to this mixture and stirred overnight during which time a bright yellow precipitate was observed to form. To this solution was added aqueous NH₄OH (50-60 mL, 28-30%), and then refluxed for 24 h. Cooling the mixture resulted in formation of a precipitate which was filtered and washed with cold CHCl₃ to yield a white solid (2.53 g, 55%). ¹H NMR (CD₃OD, 300 MHz, ppm): δ 8.68-8.71 (d, 2H, *J* = 4.8 Hz, Py-*H*^{6,6''}), 8.64-8.71 (s, 2H, Py-*H*^{3',5'}), 8.68-8.71 (d, 2H, *J* = 8.1 Hz, Py-*H*^{3,3''}), 7.97-8.03 (dt, 2H, *J* = 8.1, 1.8 Hz, Py-*H*^{4,4''}), 7.71-7.79 (d, *J* = 8.4 Hz, 4H, Ph-*H*), 7.46-7.50 (dd, 2H, *J* = 4.8, 1.8 Hz, Py-*H*^{5,5''}). MS (*m/z*): Calcd. for [C₂₁H₁₆N₃O₂B]⁺: 353.13; Found: 354.1251 [M+H].

2,6-(3'-Diterpyridine)-NDI (7): A solution of diimide **3** (0.2 g, 0.3 mmol) and boronic acid **6** (0.4 g, 0.9 mmol), together with Na₂CO₃ (5 equivs), *tert*-butyl alcohol (7 mL), and PdCl₂(PPh₃)₂

(50 mg) in, toluene (25 mL), water (25 mL) was degassed thrice and purged with N₂ in a Schlenk line and then refluxed for 24 h until the solution turned a dark purple color. After cooling to room temperature, the organic layer was extracted with CHCl₃ and dried over MgSO₄. The sample was then concentrated under vacuum and the residue chromatographed on silica with CH₂Cl₂/hexane (80:20) to result in a yellow solid (0.10 g, 33.3%). ¹H NMR (500 MHz, CDCl₃, ppm): 8.82 (s, 4H, tpy-*H*^{3',5'}), 8.74 (s, 2H, NDI-H), 8.71-8.72 (d, *J* = 2.4 Hz, 4H, tpy-*H*^{6,6''}), 8.68-8.70 (d, *J* = 4.5 Hz, 4H, tpy-*H*^{3,3''}), 8.07-8.08 (d, *J* = 8 Hz, 4H, Ph-*H*), 7.98 (s, 2H, Ph-*H*), 7.87-7.91 (t, 4H, tpy-*H*^{4,4''}), 7.69-7.72 (t, 2H, Ph-*H*), 7.61-7.55 (d, *J* = Hz, 4H, Ph-*H*), 7.34-7.37 (t, 4H, tpy-*H*^{5,5''}), 4.02-4.05 (t, 4H, N-CH₂), 1.66 (m, 9H), 1.26-1.28 (m, 20H), 0.86 (m, 6H). ¹³C NMR (125 MHz, CDCl₃, ppm): 156.46, 156.00, 150.01, 149.21, 148.72, 142.29, 137.44, 137.11, 136.52, 133.43, 130.65, 128.79, 128.14, 127.70, 127.23, 123.94, 121.59, 119.06, 117.72, 71.82. MALDI-ToF MS (*m/z*): Calcd. for [C₇₂H₆₄N₈O₄]⁺: 1105.33, found: 1105.5170. UV-Vis in CHCl₃: λ_{max} 379 nm ($\mathcal{E} = 4 \times 10^5 \text{ M}^{-1} \text{ cm}^{-1}$) and λ_{max} 254 nm ($\mathcal{E} = 7.0 \times 10^6 \text{ M}^{-1} \text{ cm}^{-1}$).

Synthesis of Polymers **5** and **7** (M = Ru²⁺, Fe²⁺, Co²⁺)

Ru(II)-Complexes of **5 and **7**:** 2,6-(4'-Diterpyridine)-NDI (**5**) (or 2,6-(3'-diterpyridine)-NDI (**7**)) was refluxed with an equimolar amount of RuCl₂(DMSO)₄ in ethylene glycol (8 mL of solvent/per mg of **5** or **7**) under N₂ for 24 h. Upon cooling to room temperature THF was added to the reaction mixture to precipitate the polymer. The precipitate was filtered and washed several times with THF to yield the corresponding red polymer in ~85% yield. UV-Vis in DMF: **5-Ru**: λ_{max} 501 nm ($\mathcal{E} = 8 \times 10^6 \text{ M}^{-1} \text{ cm}^{-1}$) and λ_{max} 378 nm ($\mathcal{E} = 1.0 \times 10^4 \text{ M}^{-1} \text{ cm}^{-1}$), **7-Ru**: λ_{max} 495 nm ($\mathcal{E} = 5.0 \times 10^6 \text{ M}^{-1} \text{ cm}^{-1}$) and λ_{max} 376 nm ($\mathcal{E} = 2.0 \times 10^4 \text{ M}^{-1} \text{ cm}^{-1}$).

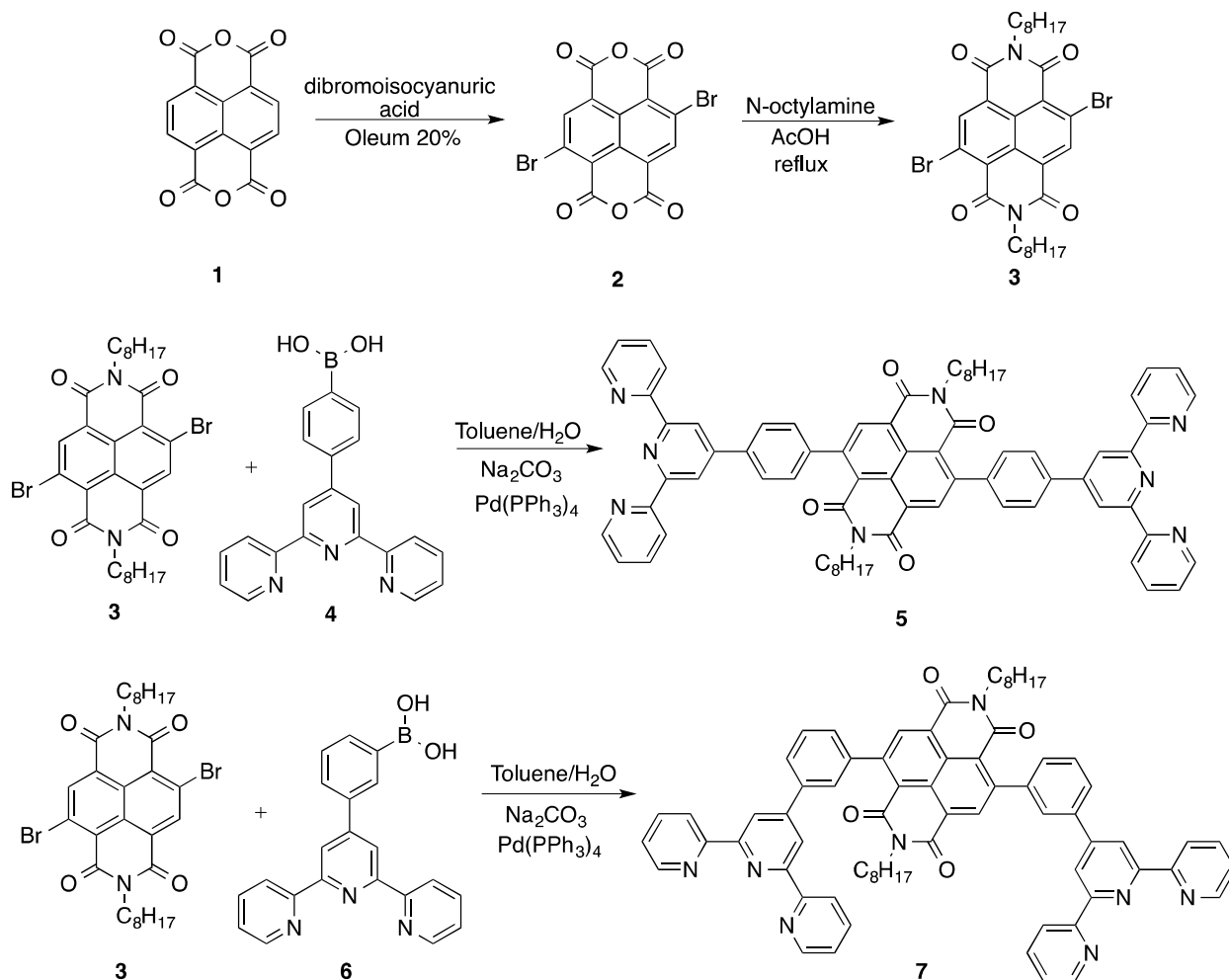
Fe(II)-Complexes of compound 5 and 7: 2,6-(4'-Diterpyridine)-NDI (**5**) (or 2,6-(3'-diterpyridine)-NDI (**7**)) was refluxed with an equimolar amount of Fe(OAc)₂ in acetic acid (8mL of solvent/mg of **5** or **7**) under N₂ for 6 h. After filtration of the reaction mixture to remove insoluble species, the solvent was removed slowly under vacuum to yield 90% of the purple iron-complex. UV-Vis (in DMF): **5-Fe**: λ_{max} 580 nm ($\mathcal{E} = 6 \times 10^5 \text{ M}^{-1} \text{ cm}^{-1}$) and λ_{max} 376 nm ($\mathcal{E} = 4.0 \times 10^4 \text{ M}^{-1} \text{ cm}^{-1}$); **7-Fe**: λ_{max} 578 nm ($\mathcal{E} = 2 \times 10^6 \text{ M}^{-1} \text{ cm}^{-1}$) and λ_{max} 378 nm ($\mathcal{E} = 3.0 \times 10^4 \text{ M}^{-1} \text{ cm}^{-1}$).

Co(II)-Complexes of 5 and 7: 2,6-(4'-Diterpyridine)-NDI (**5**) (or 2,6-(3'-diterpyridine)-NDI (**7**)) was refluxed with an equimolar amount of Co(OAc)₂ in methanol (8mL of solvent was added per mg of **5** or **7**) under N₂ for 24 h. After filtration of the reaction mixture to remove insoluble species, the solvent was removed slowly the resulting solid dried under vacuum to yield 90% of the yellow cobalt-complex. UV-Vis in DMF: **5-Co**: λ_{max} 380 nm ($\mathcal{E} = 2.0 \times 10^4 \text{ M}^{-1} \text{ cm}^{-1}$), **7-Co**: λ_{max} 380 nm ($\mathcal{E} = 1.0 \times 10^4 \text{ M}^{-1} \text{ cm}^{-1}$).

Results and Discussion

Synthesis. The synthetic route used to prepare ditopic bisterpyridines **5** and **7** is shown in Scheme 2. N,N'-Bis(n-octyl)-2,6-dibromo-1,4,5,8-naphthalenetetracarboxylic diimide (**3**)^{27,28} was synthesized from commercially available 1,4,5,8-naphthalenetetracarboxylic dianhydride. Reaction of the dibromo-NDI (**3**) with the appropriate terpyridine boronic acid (**4**²⁹ or **6**) under palladium-catalyzed Suzuki reaction conditions yielded the desired ditopic ligands in 30-40% yields after column chromatography. The ditopic monomer ligands were fully characterized by NMR and MALDI-TOF mass spectroscopy, UV-Vis absorption and cyclic voltammetry.

Scheme 2



Preparation of metallo supramolecular polymers. The polymerization of ditopic ligands (**5** and **7**) was carried out by refluxing equimolar amounts of the appropriate metal and ligand for 24 h.³⁰ For convenience, the polymers prepared from each monomer are named using the corresponding metal (Ru, Fe, and Co) together with the monomer number. The Ru(II)-metallopolymers were prepared by adding equimolar amounts of Ru(DMSO)₄Cl₂ and the ligand (**5** or **7**) in ethylene glycol under N₂ and heating. To the subsequent red solutions was added THF, resulting in precipitation of the solid polymer. The reactions to form the Co(II) and Fe(II)

analogs were performed in similar fashion using MeOH (for Co(II)) or acetic acid (for Fe(II)) as the precipitating solvents.

Absorption Spectroscopy. The optical properties of ditopic monomers **5** and **7** and the related polymers formed from **5** and **7** and Ru(II), Co(II) and Fe(II) were studied by steady state absorption and emission spectroscopies. The absorption spectra of the ligands and the metal complexes are shown in Figures 1–4, and the relevant data are presented in Table 1. The ligands are characterized by two $\pi\text{-}\pi^*$ absorption bands attributed to the terpyridine groups. The band at 287 nm for the more highly conjugated ligand **5** was considerably more intense than the higher energy band at 256 nm, whereas the low energy band for **7** appears as a shoulder at 273 nm of nearly equal intensity to the high-energy band at 254 nm. A weak and lower energy band was observed for **7** at ~ 315 nm but was not visible for **5**. The naphthalene diimide groups in both ditopic ligands are characterized by a pair of less intense bands in the $\sim 356\text{--}380$ nm range, as well as a weak broad low energy band $\sim 420\text{--}450$ nm that is attributed to a ligand-ligand charge-transfer (LLCT) absorption.

Complexation with the various metals upon polymerization leads to pronounced changes in the absorption spectra. The polymers prepared from ligand **5** have spectra that more closely resemble the corresponding metallo bis(4-phenylterpyridine) reference compounds. In contrast, the spectra for those polymers prepared from **7** have lower extinction coefficients for the low energy ligand centered (LC) $\pi\text{--}\pi^*$ transition band in the $\sim 310\text{--}325$ nm region, which are observed as weak shoulders to the red of the more intense band at $\sim 275\text{--}280$ nm. For example, **5-Ru** displays an intense LC-centered band at 316 nm, similar to the strong $\text{Ru}(\text{phtpy})_2^{2+}$ LC band at 312 nm, whereas the corresponding band in **7-Ru** is observed as a weak shoulder at ~ 314

nm. Similarly, the absorption spectra of $\text{Fe}(\text{phtpy})_2^{2+}$ and **5-Fe** both have an absorption at ~318–322 nm that is nearly absent in **7-Fe**. The absorption maxima of the NDI $\pi \rightarrow \pi^*$ transitions did not change appreciably upon complexation with any of the metals, although broadening was observed for the NDI bands in **5-Co** and **7-Co**.

In the visible region, the Ru-containing polymers displayed new absorption bands that were attributed to the allowed singlet metal-to-ligand charge-transfer ($^1\text{MLCT}$) transition at $\lambda_{\text{MLCT}} \sim 501$ nm (**5-Ru**) and ~ 495 nm (**7-Ru**), both of which were lower energy than $\text{Ru}(\text{phtpy})_2^{2+}$ (487 nm). The corresponding $^1\text{MLCT}$ bands^{31,32} in the Fe-containing polymers were also observed at lower energies ($\lambda_{\text{MLCT}} \sim 580$ nm for **5-Fe** and ~ 578 nm for **7-Fe**) than the reference $\text{Fe}(\text{phtpy})_2^{2+}$ (568 nm), consistent with other supramolecular Fe-containing polymers.³³ In general, the polymers containing the *para*-substituted ligand **5** had slightly lower energy absorption bands than the *meta*-substituted isomer **7**, consistent with the greater conjugation in the *para* isomer. Polypyridiyl complexes of Co(II) do not exhibit MLCT transitions, but sometimes exhibit weak d-d transitions in the visible region.^{5,33} These d-d transitions were too weak to observe for **5-Co** or **7-Co**, consistent with earlier work showing a decrease in the extinction coefficient of this band with the presence of conjugated electron-withdrawing groups.³³

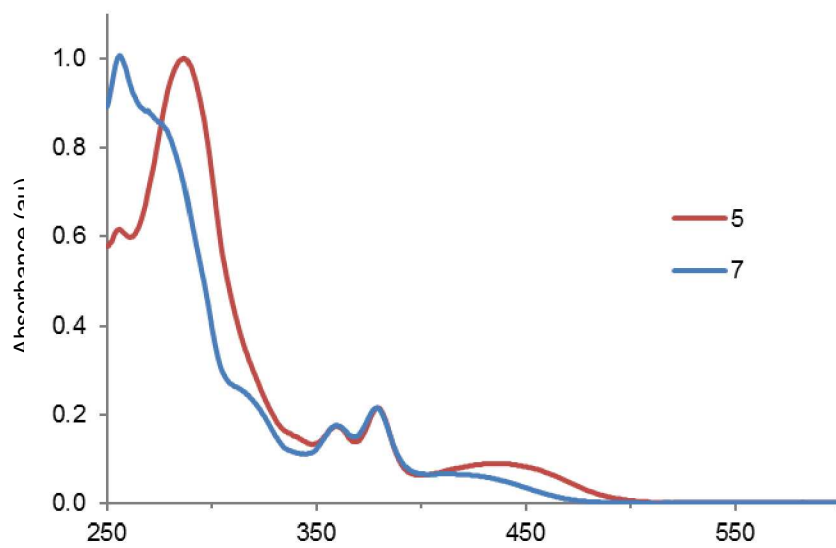


Figure 1. Normalized absorption spectra of ligands **5** and **7** in DMF.

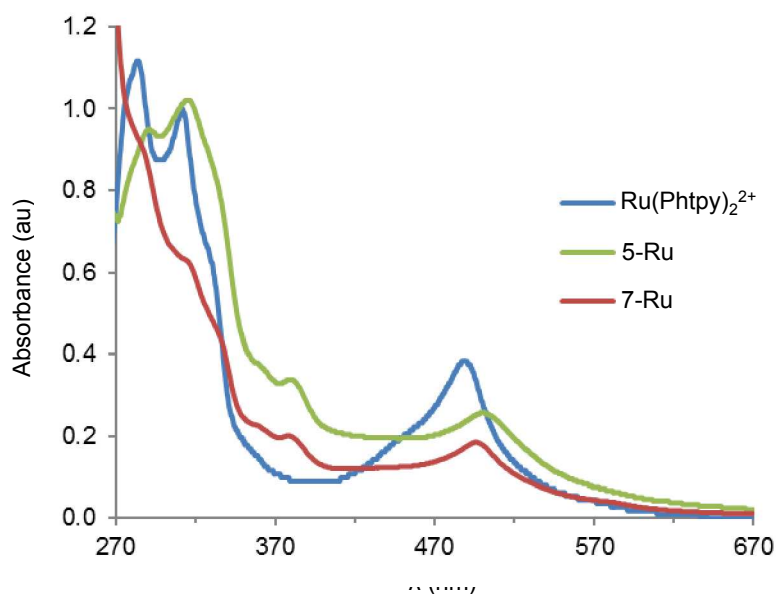


Figure 2. Normalized absorption spectra of Ru-containing terpyridine complexes **5-Ru**, **7-Ru** and Ru(phtpy)₂²⁺ in DMF.

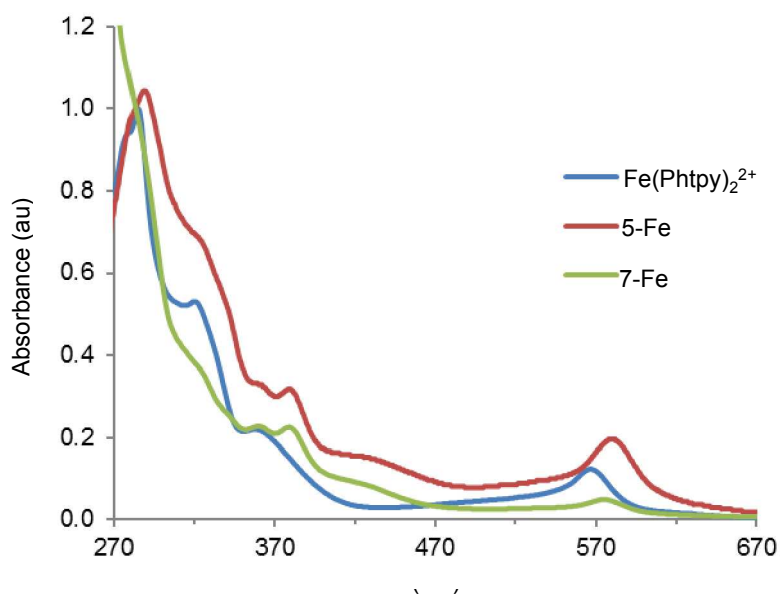


Figure 3. Normalized absorption spectra of Fe-containing terpyridine complexes **5-Fe**, **7-Fe**, and Fe(phtpy)₂²⁺ in DMF.

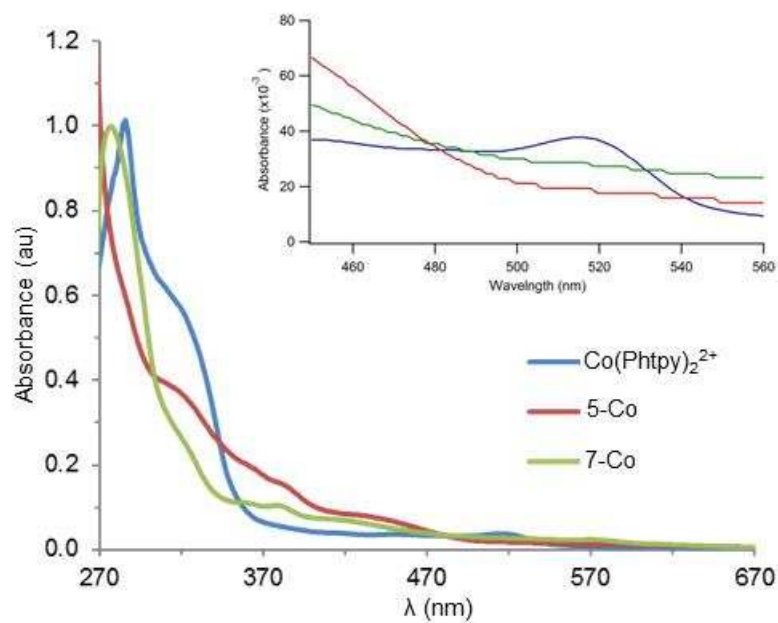


Figure 4. Normalized absorption spectra of Co-containing terpyridine complexes **5-Co**, **7-Co**, and $\text{Co}(\text{phtpy})_2^{2+}$ in DMF. The inset shows an expansion of the 450 – 560 nm region of the spectrum.

Table 1. Summary of steady-state absorption data for ditopic ligands **5** and **7**, the corresponding polymers **5-M** and **7-M** in DMF (M = Ru(II), Fe(II) and Co(II)) and the M(phtpy)₂²⁺ reference compounds in DMF.

Compound	λ_{LC} (nm)	λ_{NDI} (nm)	λ_{MLCT} (nm)
5	256, 287	380	---
5-Ru	287, 316, 335 ^a	358, 378	501
5-Fe	288, 322 ^a	358, 376	580
5-Co	275	380	---
7	254, 273 ^a	379	---
7-Ru	281, 314, ^a 336 ^a	358, 376	495
7-Fe	280, 321 ^a	358, 378	578
7-Co	276	380	---
Ru(phtpy) ₂ ^{2+,b}	282, 312, 328 ^a	---	487
Fe(phtpy) ₂ ^{2+,c}	284, 318 ^a	---	568
Co(phtpy) ₂ ^{2+,d}	286	---	516

^aObserved as a shoulder. ^bTaken from ref. 39. ^cThis work. ^dThis work as well as Wilkins, D.H.; Smith, G.F. *Anal. Chim. Acta* **1953**, *9*, 338–348.

Electrochemistry. Cyclic voltammetry (CV) measurements were performed on **5**, **7**, $\text{Ru}(\text{phtpy})_2^{2+}$, $\text{Fe}(\text{phtpy})_2^{2+}$, $\text{Co}(\text{phtpy})_2^{2+}$ and the corresponding polymers **5-M** and **7-M** in DMF. The results of these experiments are summarized in Table 2. The quasi-reversible reduction potentials for the $\text{NDI}^0/\text{NDI}^-$ and $\text{NDI}^-/\text{NDI}^{2-}$ couples for the uncomplexed ligands **5** and **7** were found to be similar to one another (-0.542 V and -0.995 V for **5**, and -0.515 V and -0.980 V for **7**). Weak irreversible oxidation waves were observed for the ligands at ~ 1.05 V (**5**) and ~ 1.02 V (**7**). The $\text{M}^{3+}/\text{M}^{2+}$ oxidation potentials (E_{ox}) of the metallo bis(phenylterpyridines) (i.e., $\text{M}(\text{phtpy})_2^{2+}$) were determined as benchmarks for **5-M** and **7-M**, and were found to be 1.27 V ($\text{M} = \text{Ru}^{2+}$), 1.05 V ($\text{M} = \text{Fe}^{2+}$) and 0.220 V ($\text{M} = \text{Co}^{2+}$) vs. the SCE.³⁴

The irreversible E_{ox} values for the $\text{M}^{3+}/\text{M}^{2+}$ couple in the polymers were also determined where possible, although kinetic issues related to the large size of these polymers and their aggregates in solution made accurate determination difficult in some cases.^{35,36} Weak E_{ox} and E_{red} were observed by increasing the scan rate for these samples. For **5-Fe**, the E_{ox} value could not be determined and the value for the $\text{Fe}(\text{phtpy})_2^{2+}$ standard was therefore used in the subsequent calculation for electron-transfer. The oxidation potential for **5-Co** (0.14 V) was slightly shifted toward lower potential than $\text{Co}(\text{phtpy})_2^{2+}$, which may indicate communication between the metal-bisterpyridine groups. The E_{ox} values for both Ru-containing polymers and **7-Fe** were relatively close to those of the $\text{M}(\text{phtpy})_2^{2+}$ standards. Finally, the NDI oxidation potential was only observed in the anodic waves for the two Co^{2+} -containing polymers, and was estimated from these values as 1.02 V for **7-Co** and 0.93 V for **5-Co**.

Table 2. Electrochemical data for ditopic ligands **5** and **7**, and the corresponding polymers **5-M** and **7-M** in DMF (M = Ru(II), Fe(II) and Co(II)).

Compound	E_{ox} (V) ^{a,b}	E_{red} (V) ^{a,b}	E_{NDI} (eV)	E_{MLCT} (eV)	HOMO (eV)	LUMO (eV)	$\Delta G_{ET/NDI}^c$ (eV)
5	1.05	-0.542	2.74	---	-7.0	-4.4	---
7	1.02	-0.515	2.66	---	-7.0	-4.4	---
Ru(phtpy)₂²⁺	1.27	---	---	1.99	-6.3	---	---
Fe(phtpy)₂²⁺	1.05	---	---	---	-6.1	---	---
Co(phtpy)₂²⁺	0.220	---	---	---	-5.2	---	---
5-Ru	1.20	-0.82	2.76	2.0 ^d	-6.2	-4.2	-0.74
5-Fe	---	---	2.77	---	---	---	---
5-Co	0.14	-0.99	2.74	---	-5.1	-4.0	-1.61
7-Ru	1.20	-0.80	2.77	2.0 ^d	-6.2	---	-0.77
7-Fe	1.02	-0.97	2.76	---	-7.0	-4.0	-0.77
7-Co	0.22	-1.10	2.74	---	-5.2	-3.9	-1.42

^aValues were determined in DMF with 0.1 M TBAPF₆ as the supporting electrolyte, Ag/AgClO₄ reference electrode and a gold working electrode. ^bReferenced to the SCE using the conversion: $E(SCE) = E(Ag/AgClO_4) + 0.42$ (Howell, J.O.; Goncalves, J.M.; Amatore, C.; Klasinc, L.; Wightman, R.M.; Kochi, J. K. *J. Am. Chem. Soc.* **1984**, *106*, 3968–3976.; Connelly, N.G.; Geiger, W.E. *Chem. Rev.* **1996**, *96*, 877–9110). ^cCalculated using the equation: $\Delta G_{ET} = E_{ox}(M^{3+/2+}) - E_{red}(NDI/0) - E_{NDI}$. ^dTaken from Alemán, E.A.; Shreiner, C.D.; Rajesh, C.S.; Smith, T.; Garrison, S.A.; Modarelli, D.A. *Dalton Transactions* **2009**, 6562 – 6567.

Emission Properties. Room temperature steady state emission measurements were performed on monomeric ligands **5** and **7**, complexes $\text{Ru}(\text{phtpy})_2^{2+}$, $\text{Fe}(\text{phtpy})_2^{2+}$, $\text{Co}(\text{phtpy})_2^{2+}$, and polymers **5/7-Ru**, **5/7-Fe** and **5/7-Co**. Excitation of **5** and **7** was performed at the NDI maximum ($\lambda_{\text{ex}} \sim 380$ nm), while those of the polymers were performed at both the NDI and metal-bisterpyridine absorption maxima. For monomers **5** and **7**, excitation of the NDI groups at $\lambda_{\text{ex}} 380$ nm resulted in strong emission signals with maxima at 525 nm (**5**) and 556 nm (**7**), yielding fluorescence quantum yields (Φ_{F}) of 0.41 (**5**) and 0.56 (**7**), consistent with the fluorescence properties of other 2,6-diaryl substituted NDIs.³⁷ Excitation of the $\text{M}(\text{phtpy})_2^{2+}$ reference compounds into the LC, MLCT or d-d absorption bands resulted in spectra that were too weak to accurately determine the Φ_{em} values, consistent with the short-lived $\text{M}(\text{tpy})_2^{2+}$ excited states.^{38,39,40,41,42}

The excited state energies of the NDI group in **5** and **7** were measured using the NDI absorption maxima and emission minima, and were determined to be 2.74 eV (**5**) and 2.66 eV (**7**), similar to other 2,6-diaryl substituted NDIs.¹³ Incorporation of the metal in the metallopolymers results in slightly higher values for the NDI excited singlet energy ($\sim 2.75 - 2.77$ eV).⁴³ The excited state energies, together with the redox potentials reported in Table 2, were used to calculate the free energies of electron transfer (ΔG_{ET} , Table 2).

Excitation of the metal-bisterpyridine groups in the polymeric samples did not result in appreciable emission at either room temperature or at 77K. Similarly, excitation of the NDI groups in the polymers ($\lambda_{\text{ex}} \sim 380$ nm) did not result in emission at either temperature, indicating the NDI excited state was completely or nearly completely quenched relative to the spectra of monomeric ligands **5** and **7**. Because the major difference between the ditopic NDI-containing ligands **5** and **7** and the metallopolymers is complexation of the ligand with the various metals,

the quenching of the NDI fluorescence in the metallopolymers with NDI excitation can therefore attributed to either (1) intramolecular electron-transfer from the $M(\text{phtpy})_2^{2+}$ groups to the excited NDI, producing the $M(\text{phtpy})_2^{3+}$ -NDI $^-$ charge-separated states, or (2) energy-transfer from the excited NDI group to generate the excited state of the non-emissive $M(\text{tpy})_2^{2+}$ groups. Based on prior experiments with $M(\text{tpy})_2^{2+}$ -acceptor dyads,^{39,44} and in the absence of transient absorption data, we assume electron-transfer is the cause of the decrease in the NDI emission.

Surface Morphologies. In order to investigate the morphologies of the polymers prepared in this work, atomic force microscopy (AFM), transmission electron microscopy (TEM), and scanning electron microscopy (SEM) were performed on each sample. Rod-like structures were observed for the *para*-substituted **5-Ru** polymers using all three techniques (Figure 5). These structures were observed to have an average length (along the z-axis) of $\sim 4\text{--}8\ \mu\text{m}$, with nearly square ends having xy-dimensions averaging $0.3\text{--}0.4\ \mu\text{m}$. MM2 calculations^{45,46} of **5-Ru** predict an approximate molecular width of $\sim 2.6\ \text{nm}$, indicating $\sim 115\text{--}155$ polymer chains are stacked in the xy-directions to form the nanorods.

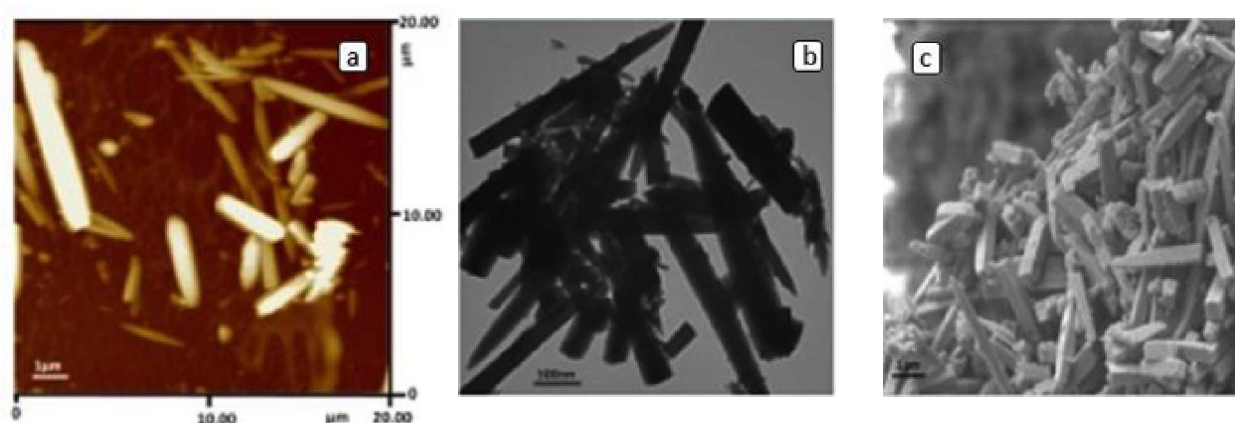


Figure 5. Typical AFM (a), TEM (b) and SEM (c) images of **5-Ru** showing the rod-shaped structures formed upon deposition onto a solid support.

The iron-containing polymers **5-Fe** were also observed to assemble into rod-like morphologies by TEM and AFM, although these structures were less distinct and showed greater amounts of aggregation between individual rods. Based on the TEM images, the length of the polymers in these polymers was estimated to be $\sim 0.5\text{--}0.8\ \mu\text{m}$. The **5-Co** polymers also formed significantly shorter rod-like structures that were observed to aggregate into larger cluster-like morphologies that are attributed to the shorter polymer lengths. The significantly greater lengths observed for the $\text{Ru}(\text{tpy})_2^{2+}$ -containing polymers compared to the Co^{2+} or Fe^{2+} containing polymers is likely a result of the greater binding constant inherent in ruthenium bisterpyridines.

Surprisingly, the **7-Ru** polymers derived from the *meta*-substituted ditopic ligand (**7**) also displayed a rod-like morphology, although the average length of these polymers was measured to be $\sim 1\text{--}2\ \mu\text{m}$, significantly shorter than those observed for *para*-substituted **5-Ru**. The **7-Fe** and **7-Co** polymers appeared as spherical structures in SEM experiments, while thin, fiber-like structures were observed by TEM and AFM for both polymers, with lengths on the order of $\sim 0.2\text{--}2\ \mu\text{m}$. Based on this data, it is clear the morphology is highly dependent upon the regiochemistry of the ditopic ligand as well as the nature of the metal center, with the **5-M** polymers assembling into longer rod-like morphologies, while the **7-M** polymer morphologies displayed shorter assemblies with more random aggregation patterns.

Conclusions

In this work, *para* (linear) and *meta* (bent) core-substituted naphthalene diimide spacer groups were incorporated into self-assembled metallo (Ru(II), Fe(II), Co(II)) bisterpyridine self-assembled polymers. The morphologies, photophysical and electrochemical properties of each polymer were then explored as a function of the metal and NDI regiochemistry. Experiments on the reference compounds **5** and **7** indicate that substitution on the core of the naphthalene diimide has only a mild impact on the photophysical and electrochemical properties of the NDI group. Metal complexation leads to a significant decrease of the NDI emission in all metallopolymer compared to the reference compounds **5** and **7**, most likely as a result of electron-transfer from the metallo bis(terpyridine) to the excited NDI group. Although photophysical differences were observed among the different metal complexes, the differences between the two regiopolymers (i.e., **5-M** vs **7-M**) were minor. A significantly greater effect was observed between the two ligands upon analysis of the polymer morphologies. Polymers prepared from the *para*-substituted (linear) regioisomer **5** were observed to form substantially longer and thicker fibers. These results are directly attributed to the linear nature of the *para*-substituted polymer. The *meta*-substituted polymer is expected to coil or have a disordered structure, and therefore should not undergo inter-chain stacking as efficiently as the *para* isomer. Lengths on the order of $\sim 8 \mu\text{m}$ were observed for the bundle of the longest polymers (**5-Ru**).

Acknowledgements

D.A.M. gratefully acknowledges the support of the National Science Foundation (NSF-1412362) and The University of Akron. J.M.M. gratefully acknowledges the support of the National Science Foundation (MRI-1039259). D.A.M. and R.A. acknowledge generous support

from King Abdulaziz City for Science and Technology (KACST-01480/535214). We also thank Mr. Lucas McDonald for help with low temperature emission experiments.

Notes and references

‡Department of Chemistry and The Center for Laser and Optical Spectroscopy, Knight Chemical Laboratory, The University of Akron, Akron, Ohio 44325-3601, United States

§Department of Chemistry and Biochemistry, Hiram College, Hiram, Ohio 44234, United States

†Petrochemicals Research Institute, King Abdulaziz City for Science and Technology, P.O. Box 6086, Riyadh 11442, Saudi Arabia

Electronic Supplementary Information (ESI) available: Steady state fluorescence spectra of **5** and **7**, atomic force microscopy (AFM), transmission electron microscopy (TEM) and scanning electron microscopy (SEM) data are shown.

¹M. Higuchi *Polym. J.* 2009, **41**, 511–520.

²U. Mansfeld, A. Winter, M.D. Hager, W. Günther, E. Altuntaş, U.S. Schubert *J. Polym. Sci. Part A Polym. Chem.* 2013, **51**, 2006–2015.

³M. Burnworth, D. Knapton, S.J. Rowan, C. Weder *J. Inorg. Organomet. Polym. Mater.* 2007, **17**, 91–103.

⁴F.S. Han, M. Higuchi, T. Ikeda, Y. Negishi, T. Tsukuda, D.G. Kurth *J. Mater. Chem.* 2008, **18**, 4555–4560.

⁵F.S. Han, M. Higuchi, D.G. Kurth *Adv. Mater.* 2007, **19**, 3928–3931.

⁶Y. Yan, J. Huang *Coord. Chem. Rev.* 2010, **254**, 1072–1080.

⁷Y. Liu, Z. Wang, X. Zhang *Chem. Soc. Rev.* 2012, **41**, 5922–5932.

⁸M. Chipper, M.A.R. Meier, J.M. Kranenburg, U.S. Schubert *Macromol. Chem. Phys.* 2007, **208**, 679–689.

⁹J. Yuan, H. Zhang, G. Hong, Y. Chen, G. Chen, Y. Xu, W. Weng *J. Mater. Chem. B* 2013, **1**, 4809–4818.

¹⁰J.P. Collin, S. Guillerez, J.P. Sauvage, F. Barigelletti, L. De Cola, L. Flamigni, V. Balzani *Inorg. Chem.* 1991, **30**, 4230–4238.

¹¹H.J. Bolink, L. Cappelli, E. Coronado, P. Gaviña *Inorg. Chem.* 2005, **44**, 5966–5968.

¹²A. Wild, A. Winter, M.D. Hager, H. Görls, U.S. Schubert *Macromol. Rapid Commun.* 2012, **33**, 517–521.

¹³N. Sakai, J. Mareda, E. Vauthey, S. Matile *Chem. Commun.*, 2010, **46**, 4225–4237.

¹⁴S. Shin, E. Chang, S. Lee, J.K. Cho, K.-U. Jeong *Thin Solid Films* 2011, **520**, 486–490.

- ¹⁵J. Chang, Q. Ye, K.-W. Huang, J. Zhang, Z.-K. Chen, J. Wu, C. Chi *Org. Lett.* 2012, **14**, 2964–2967.
- ¹⁶C.R. Wade, M. Li, M. Dincă *Angew. Chem. Int. Ed. Engl.* 2013, **52**, 13377–13381.
- ¹⁷S.V. Bhosale, M.B. Kalyankar, S.J. Langford *Org. Lett.* 2009, **11**, 5418–5421.
- ¹⁸S.V. Bhosale, C.H. Jani, S.J. Langford, S. J. *Chem. Soc. Rev.* 2008, **37**, 331–342.
- ¹⁹Y. Posokhov, S. Alp, B. Koez, Y. Dilgin, S. Icli *Turk. J. Chem.* 2004, **28**, 415–424.
- ²⁰G. Andric, J.F. Boas, A.M. Bond, G.D. Fallon, K.P. Ghiggino, C.F. Hogan, J.A. Hutchison, M.A.-P. Lee, S.J. Langford, J.R. Pilbrow, G.J. Troup, C.P. Woodward *Aust. J. Chem.* 2004, **57**, 1011–1019.
- ²¹M.-J. Lin, Á. J. Jiménez, C. Burschka, F. Würthner *Chem. Commun.* 2012, **48**, 12050–12052.
- ²²S.V. Bhosale, M.B. Kalyankar, S.V. Bhosale, S.J. Langford, E.F. Reid, C.F. Hogan *New J. Chem.* 2009, **33**, 2409–2413.
- ²³H. Shao, J. Seifert, N.C. Romano, M. Gao, J.J. Helmus, C.P. Jaronec, D.A. Modarelli, J.R. Parquette *Angew. Chem.*, 2010, **49**, 7688–7691.
- ²⁴S. Tu, S.H. Kim, J. Joseph, D.A. Modarelli, J.R. Parquette *J. Am. Chem. Soc.* 2011, **133(47)**, 19125–19130.
- ²⁵C. Peebles, R. Piland, B.L. Iverson *Chem. Eur. J.*, 2013, **19**, 11598–11602.
- ²⁶G. Schwarz, T.K. Sievers, Y. Bodenthin, I. Hasslauer, T. Geue, J. Koetz, D. G. Kurth *J. Mater. Chem.* 2010, **20**, 4142–4148.
- ²⁷M. Sasikumar, Y.V. Suseela, T. Govindaraju *Asian J. Org. Chem.* 2013, **2**, 779–785.
- ²⁸C. Thalacker, C. Röger, F. Würthner, F. *J. Org. Chem.* 2006, **71**, 8098–8105.
- ²⁹J.-L. Wang, X. Li, X. Lu, I.-F. Hsieh, Y. Cao, C.N. Moorefield, C. Wesdemiotis, S.Z.D. Cheng, G.R. Newkome *J. Am. Chem. Soc.* 2011, **133**, 11450–11453.
- ³⁰Y. Muronoi, J. Zhang, M. Higuchi, H. Maki *Chem. Lett.* 2013, **42**, 761–763.
- ³¹J.K. McCusker, K.N. Walda, R.C. Dunn, J.D. Simon, D. Magde, D.N. Hendrickson *J. Am. Chem. Soc.* 1993, **115**, 298–307.
- ³²T.G. Spence, B.T. Trotter, L.A. Posey *J. Phys. Chem. A* 1998, **102**, 7779–7786.
- ³³D.G. Kurth, M. Schütte, J. Wen *Colloids Surfaces A Physicochem. Eng. Asp.* 2002, **198–200**, 633–643.
- ³⁴D. Chen, P.-L. Fabre, O. Reynes *Electrochim. Acta* 2011, **56**, 8603–8610.
- ³⁵S. Bernhard, K. Takada, D.J. Díaz, H.D. Abruña, H. Mürner *J. Am. Chem. Soc.* 2001, **123**, 10265–10271.
- ³⁶R. Dobrawa, F. Würthner *Chem. Commun.* 2002, 1878–1879.
- ³⁷S.V. Bhosale, M. Kalyankar, S.V. Bhosale, S.J. Langford, E. Reid, C. Hogan, C. *New J. Chem.* 2009, **33**, 2409–2413.
- ³⁸O. Johansson, M. Borgström, R. Lomoth, M. Palmblad, J. Bergquist, L. Hammarström, L. Sun, B. Åkermark *Inorg. Chem.* 2003, **42**, 2908–2918.
- ³⁹Alemán, E.A.; Shreiner, C.D.; Rajesh, C.S.; Smith, T.; Garrison, S.A.; Modarelli, D.A. *Dalton Trans.* 2009, 6562–6577.
- ⁴⁰Brown, A.M.; McCusker, C.E.; McCusker, J.K. *Dalton Trans.*, 2014, **DOI: 10.1039/C4DT02849J**.
- ⁴¹Yoon, Z.S.; Chan, Y.-T.; Li, S.; Newkome, G.R.; Goodson III, T. *J. Phys. Chem. B* 2010, **114**, 11731–11736.
- ⁴²Sauvage, J.-P.; Collin, J.-P.; Chambron, J.-C.; Guillerez, S.; Coudret, C.; Balzani, V.; Barigelletti, F.; De Cola, L.; Flamigni, L. *Chem. Rev.* 1994, **94**, 993–1019.

⁴³ No emission was observed from the polymeric samples upon NDI excitation, and the E_{NDI} energies in the polymers were therefore estimated using the E_{NDI} values for **5** and **7** and adjusting slightly to account for the change in absorption maxima. The estimated values represent upper limits.

⁴⁴ M. Falkenström, S. Ott, R. Lomoth, J. Bergquist, L. Hammarström, O. Johansson *Inorg. Chem.*, 2006, **45**, 4820–4829; M. Falkenström, O. Johansson, L. Hammarström *Inorg. Chim. Acta*, 2007, **360**, 741–750.; O. Johansson, M. Borgström, R. Lomoth, M. Palmblad, J. Bergquist, L. Hammarström, L. Sun, B. Åkermark *Inorg. Chem.*, 2003, **42**, 2908–2918.

⁴⁵ R. Dobrawa, F. Würthner, F. *Chem. Commun.* 2002, 1878–1879.

⁴⁶ R. Dobrawa, M. Lysetska, P. Ballester, M. Grüne, F. Würthner *Macromolecules* 2005, **38**, 1315–1325.